MICROSCOPIC CALCULATIONS OF NUCLEAR AND NEUTRON MATTER, SYMMETRY ENERGY AND NEUTRON STARS*

S. Gandolfi

Theoretical Division, Los Alamos National Laboratory
Los Alamos, NM, 87545, USA

(Received January 12, 2015)

We present Quantum Monte Carlo calculations of the equation of state of neutron matter. The equation of state is directly related to the symmetry energy and determines the mass and radius of neutron stars, providing then a connection between terrestrial experiments and astronomical observations. We also show preliminary results of the equation of state of nuclear matter.

DOI:10.5506/APhysPolB.46.359
PACS numbers: 21.65.Mn, 26.60.Kp, 26.60.–c

1. Introduction

The study of homogeneous dense nuclear and neutron matter from a microscopic point of view is important for several reasons. Although these systems cannot be directly realized in terrestrial experiments (*i.e.* it is not possible to measure the equation of state, response functions, and other properties), they are intimately related to other systems of interests. The saturation point of isospin symmetric nuclear matter can be extrapolated from properties of heavy nuclei, *i.e.* the saturation density is about 0.16 fm^{-3}, and its energy per nucleon is about -16 MeV. The equation of state should be in principle calculated using the same nuclear Hamiltonian used to study properties of nuclei, and a still open question is whether the same nuclear interactions can simultaneously describe properties of nuclei and the saturation of nuclear matter.

* Presented at the Zakopane Conference on Nuclear Physics "Extremes of the Nuclear Landscape", Zakopane, Poland, August 31–September 7, 2014.

On the other hand, the equation of state of pure neutron matter is a very good approximation to model neutron stars around nuclear densities, in particular to calculate the maximum mass and radius. The symmetry energy can be simply defined as the difference between the nuclear matter and neutron matter energy, and gives the energy cost of the isospin-asymmetry in the homogeneous nucleonic matter. We will define $E_{\rm sym}$ the symmetry energy at nuclear saturation density $\rho_0 = 0.16$ fm^{-3}. In the last few years, the study of $E_{\rm sym}$ and its slope L has received considerable attention (see for example, Ref. [1] for a recent experimental/theoretical review). The role of the symmetry energy and its slope is essential to understand the mechanism of stability of very neutron-rich nuclei, and is also related to many phenomena occurring in neutron stars. Because of β-decay processes, a small fraction of protons, about 10%, is present inside neutron stars, but their role in the structure is very small (although they are instead very important for cooling and other processes). The inner crust of neutron stars, where the density is a fraction of nuclear densities, is mostly composed of neutrons surrounding a matter made of extremely-neutron rich nuclei that, depending on the density, may exhibit very different phases and properties. The extremely rich phase diagram of crustal matter is strongly related to the role of $E_{\rm sym}$. For example, it governs the phase-transition between the crust and the core [2, 3] and the nature of r-mode instabilities [4, 5].

The nuclear interaction between neutrons is simpler, as the tensor force, that is dominant in $T = 0$, is very weak in $T = 1$ (T is the isospin of the nucleon–nucleon pair). Unfortunately, there is no direct experiment to measure properties of either homogeneous or inhomogeneous neutron matter. Some properties can be extracted by extrapolating to very large isospin-asymmetry, but such extrapolations are always model dependent. For all the above reasons, the calculation of the equation of state of pure neutron matter is particularly challenging.

In the last few decades, properties of nuclear systems have been successfully described by nucleon–nucleon potentials like Argonne and three-body Urbana/Illinois interactions, that reproduce two-body scattering data and properties of light nuclei with very high precision [6–8]. Using very accurate many-body techniques, it has been shown that those nuclear Hamiltonians can reproduce several properties of light nuclei extremely well, including binding energies of ground- and excited-states, radii, matrix elements, scattering states, and other observables [9–12]. Another approach to model the nucleon–nucleon interaction is provided within the framework of chiral effective field theory (EFT). In this approach, the diagrams describing the interaction (through the exchange of pions) are systematically organized by expanding over momenta (referred to some momentum scale). Both the Argonne and the chiral interactions requires non-perturbative many-body

techniques to calculate the ground state properties. In this paper, we will present results obtained using a correlated wave function combined with Quantum Monte Carlo (QMC) methods, that have provided highly accurate solutions of the ground state of many-body nuclear systems [13].

2. The nuclear Hamiltonian and quantum Monte Carlo

In our model, neutrons are non-relativistic point-like particles interacting via two- and three-body potentials:

$$H = \sum_{i=1}^{A} \frac{p_i^2}{2m} + \sum_{i<j} v_{ij} + \sum_{i<j<k} v_{ijk}\,. \tag{1}$$

The two body-potential that we use is the Argonne AV8′ [14], that is a simplified form of the Argonne AV18 [6]. Although simpler to use in QMC calculations, AV8′ provides almost the same accuracy as AV18 in fitting nucleon–nucleon (NN) scattering data. The three-body force is not as well constrained as the NN interaction, but its inclusion in realistic nuclear Hamiltonians is important to correctly describe the binding energy of light nuclei.

The Urbana IX (UIX) three-body force has been originally proposed in combination with the Argonne AV18 and AV8′ [15]. Although it slightly underbinds the energy of light nuclei, it has been extensively used to study the equation of state of nuclear and neutron matter [16–18]. The Illinois forces have been introduced to improve the description of both ground- and excited-states of light nuclei, showing an excellent accuracy [7, 9, 19], but it produces an unphysical overbinding in pure neutron systems [20, 21].

Another class of nucleon–nucleon potentials are derived within chiral effective field theory. In this approach, the relevant diagrams entering in the nucleon–nucleon interaction are systematically organized in powers of Q/Λ, where Q is of the order of typical momenta of nucleons, and Λ is a momentum cutoff where the chiral EFT expansion is expected to break down. The long-range terms entering into the chiral EFT potentials are fully determined by π-nucleon scattering data, while the parameters associated with the contact terms are obtained by fitting low-energy scattering data, typically up to lab energies of about 100–200 MeV. For more details, see Refs. [22, 23]. Generally, these interactions have strong non-local terms, and, as a consequence, they cannot be easily included in QMC calculations. Recently, it has been shown that these potentials can be designed to be local, and combined with QMC simulations [24, 25]. However, the need to include a cutoff of the nucleon's momentum limits the applicability of chiral forces to study dense neutron matter. The cutoff of these potentials

can be controlled in a many-body calculation [24, 25]. In addition, chiral EFT naturally predicts, at each chiral order, the presence of many-body forces. For example, at next-to-next-to-leading-order (N^2LO), three-body interactions start to appear, and at the next order (N^3LO) even four-body forces are predicted.

The main advantage of Argonne interactions is that they fit nucleon–nucleon scattering data up to higher energies, and thus are better suited to study dense matter. However, nuclear interactions derived within the chiral EFT can be systematically improved (by increasing the chiral order). In addition, by changing the cutoff used to regulate the short-range parts, it is possible to study the systematic uncertainties and understand how those evolve from few- to many-body systems.

We solve the many-body ground-state with a projection in imaginary-time, *i.e.*

$$\Psi(\tau) = \exp[-H\tau]\Psi_{\rm v}\,, \tag{2}$$

where $\Psi_{\rm v}$ is a variational ansatz, and H is the Hamiltonian of the system. In the limit of $\tau \to \infty$, Ψ approaches the ground-state of H. The evolution in imaginary-time is performed by sampling configurations of the system using Monte Carlo techniques, and expectation values are evaluated over the sampled configurations. The main difference between the well know Green's Function Monte Carlo (GFMC) and the Auxiliary Field Diffusion Monte Carlo (AFDMC) used here is in the way that spin/isospin states are treated. In GFMC, all the spin/isospin states are explicitly included in the variational wave function. The results obtained are very accurate but limited to the ^{12}C [9, 19, 26] or 16 neutrons [27]. The AFDMC method samples the spin/isospin states using the Hubbard–Stratonovich transformation rather than summing them explicitly [28]. The calculation can be then extended up to many neutrons, making the simulation of homogeneous matter and heavy nuclear systems possible. The AFDMC has proven to be very accurate when compared to GFMC calculation of energies of neutrons confined in an external potential and for light nuclei [27, 29].

3. The equation of state of neutron matter

There are several reasons to focus on pure neutron matter in addition to those mentioned before. The three-body interaction is non-zero only in the $T = 3/2$ isospin-channel (T is the total isospin of three-nucleons), while in the presence of protons there are also contributions in $T = 1/2$. The latter term is dominant in nuclei, and then the $T = 3/2$ is thus only weakly accessible by studying properties of nuclei.

We present several equations of state obtained using different models of the three-neutron force in Fig. 1, see the caption for the descriptions of the various results. The effect of using different models of the three-neutron force is clear in the two bands, where the high density behavior is shown up to about $3\rho_0$. At such high density, the various models giving the same symmetry energy at saturation produce an uncertainty in the energy per neutron of about 20 MeV. The parametrizations of the equation of state obtained from different nuclear Hamiltonians are given in Refs. [18, 30].

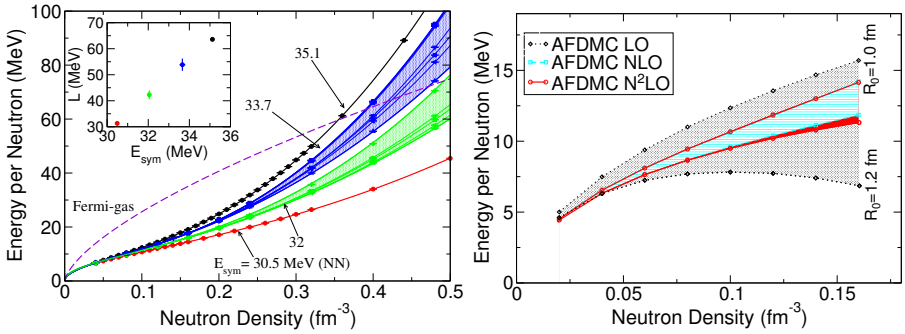

Fig. 1. The equation of state of neutron matter calculated using AFDMC for various Hamiltonians. In the left panel, the lower (red) curve is obtained by including the NN alone, and the higher (black) one is obtained by adding the Urbana IX three-body force. The light grey (green) and dark grey (blue) bands correspond to equation of states with the same $E_{\rm sym}$ (32 and 33.7 MeV respectively), obtained with several models of three-neutron forces combined with AV8′. In the inset, we show the value of L as a function of $E_{\rm sym}$ obtained by fitting the equation of state. The figure is taken from Ref. [18]. In the right panel, we show the results obtained with nucleon–nucleon chiral EFT Hamiltonians at LO, NLO and N^{2}LO. The bands correspond to the results obtained by changing the cutoff R_0 from 1 to 1.2 fm as indicated in the figure. The figure is adapted from Ref. [24].

At density ρ_0, symmetric nuclear matter saturates, and we can extract the value of $E_{\rm sym}$ and L directly from the pure neutron matter equation of state. The result of fitting the pure neutron matter equation of state is shown in the inset of Fig. 1. The error bars are obtained by taking the maximum and minimum value of L for a given $E_{\rm sym}$, and the curves obtained with NN and NN+UIX are thus without error bars. From the plot, it is clear that within the models we consider, the correlation between L and $E_{\rm sym}$ is linear and quite strong.

The equation of state has been also calculated using nucleon–nucleon interactions obtained from chiral EFT at leading order (LO), NLO and N^{2}LO and with different values of the cutoff. The results are shown in the right

panel of Fig. 1. In this case, it is clear that the chiral expansion is probably converging, *i.e.* the results at N^{2}LO are compatible with those at NLO and LO. However, we should note that the three-body interactions are not included in the calculation, thus the equation of state at N^{2}LO is incomplete, and should be considered as preliminary. However, we also note that the NLO and N^{2}LO results with two-nucleon potential alone are very similar to those obtained by considering the AV8′ alone. The complete calculation at N^{2}LO including three-neutron forces is in progress, and will be published in a separate paper [31].

4. Connection to neutron star masses and radii

When the equation of state of the neutron star matter is specified, the structure of a neutron star can be calculated by integrating the Tolman–Oppenheimer–Volkoff (TOV) equations. Although other degrees of freedom, like hyperons, may form at higher densities, see for example [32], the radius of neutron stars is almost completely determined by the equation of state around nuclear densities. Here, we consider the neutron star as composed solely by neutrons, and then use the results presented in the previous section.

The neutron star mass measurements which provide the strongest constraints on the equation of state are those which have the highest mass. Recent observations [33, 34] have found two neutron stars with masses near $2M_\odot$. These two data points provide some of the strongest constraints on the nature of neutron matter above the nuclear saturation density. We begin by examining what can be deduced about the M–R relation directly from these mass measurements, without employing a separate model for high-density matter.

The mass of a neutron star as a function of its radius is shown in Fig. 2. The two bands correspond to the result obtained using the two sets of equations of state giving the same value of $E_{\rm sym}$ indicated in the figure (the colors correspond to the results of Fig. 1). As in the case of the equation of state, it is clear that the main source of uncertainty in the radius of a neutron star with $M = 1.4M_\odot$ is due to the uncertainty of $E_{\rm sym}$ rather than the model of the three-neutron force. The addition of a small proton fraction would change the radius R only slightly [16, 35], smaller than other uncertainties in the equation of state that we have discussed. In the figure, we also indicate (with the orange lines) the density of the neutron matter inside the star. Even at large masses, the radius of the neutron star is mainly governed by the equation of state of neutron matter between 1 and 2 ρ_0 [36].

The AV8′ Hamiltonian alone does not support the recent observed neutron star with a mass near $2M_\odot$ [33]. However, adding a three-body force to AV8′ can provide sufficient repulsion to be consistent with all of the constraints [18]. There is a clear correlation between neutron star radii and the

symmetry energy which determines the equation of state of neutron matter between 1 and 2 ρ_0. Within this model, from astrophysical observations, it is possible to constrain the value of $E_{\rm sym}$ and L, see, for example, Ref. [37, 38]. The results in Fig. 2 also show that the most modern neutron matter equation of state imply a maximum neutron star radius not larger than about 13 km, unless a drastic repulsion sets in just above the saturation density.

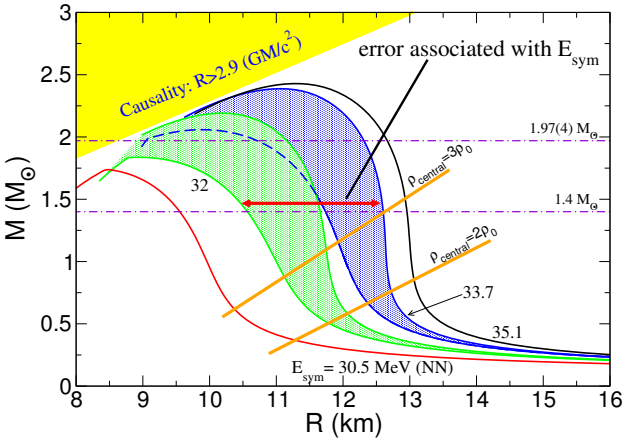

Fig. 2. The mass–radius relation of neutron stars obtained from the equations of state calculated using QMC. The various colors represent the M–R result obtained from the corresponding results described in Fig. 1. The two horizontal lines show the value of $M = 1.4$ and $1.97(4) M_\odot$ [33]. The figure is adapted from Refs. [18, 30].

5. Nuclear matter

The AFDMC method has been recently extended to calculate properties of medium nuclei and nuclear matter [29] using the nucleon–nucleon AV6′ and AV7′ interactions. Those interactions are obtained from AV8′ by dropping the two spin–orbit LS operators (AV6′), and the LS-τ (AV7′). Although they do not accurately describe the scattering data as the AV18 and AV8′, they can be exactly included into the AFDMC method. However, the AV7′ interaction described nucleon–nucleon phase shifts fairly well up to laboratory energies of about 250–300 MeV.

In the left panel of Fig. 3, we show the nuclear matter equation of state calculated using the AV6′ and AV7′ interactions. Clearly, the equation of state is quite dependent on the nucleon–nucleon interaction, and the saturation point, indicated by the diamond (blue), is not reproduced. However, we stress that three-body forces are not included in the calculations. It is quite interesting to compare with the case of pure neutron matter shown in the right panel of Fig. 3. In the case of neutrons, the AV8′ interaction is

identical to AV7′. As we can see, the equation of state obtained with AV7′ and AV6′ is quite similar, while for nuclear matter the results are quite different. This is probably due to the nucleon–nucleon phase shifts that are fitted quite differently for the two interactions. We anticipate that using chiral potentials the qualitative behavior is quite similar, and the results will be published in a future paper.

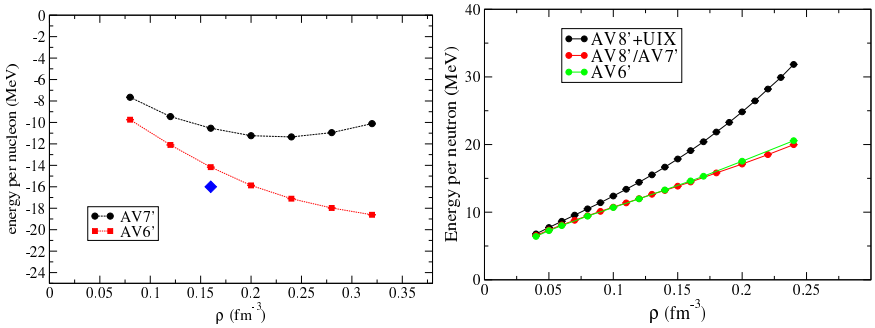

Fig. 3. Left panel: the equation of state of nuclear matter calculated using the AV6′ (lower red curve) and AV7′ (higher black curve) NN interactions [29]. The diamond (blue) shows the saturation point extrapolated from heavy nuclei. In the right panel, we show the equation of state of pure neutron matter obtained using the same Hamiltonians (grey/red and light grey/green lines), and with the addition of the UIX three-neutron force.

The author would like to thank Joel Lynn for critical comments on the manuscript. This work is supported by the U.S. Department of Energy, Office of Nuclear Physics, by the NUCLEI SciDAC program and by the LANL LDRD program. Computational resources have been provided by Los Alamos Open Supercomputing. This research used also resources of the National Energy Research Scientific Computing Center (NERSC), which is supported by the Office of Science of the U.S. Department of Energy under Contract No. DE-AC02-05CH11231.

REFERENCES

[1] M.B. Tsang *et al.*, *Phys. Rev.* **C86**, 015803 (2012).
[2] W.G. Newton, M. Gearheart, B.-A. Li, *Astrophys. J. Suppl.* **204**, 9 (2013).
[3] A.W. Steiner, S. Gandolfi, F.J. Fattoyev, W.G. Newton, *Phys. Rev.* **C91**, 015804 (2015).
[4] De-Hua Wen, W.G. Newton, Bao-An Li, *Phys. Rev.* **C85**, 025801 (2012).
[5] I. Vidaña, *Phys. Rev.* **C85**, 045808 (2012).

[6] R.B. Wiringa, V.G.J. Stoks, R. Schiavilla, *Phys. Rev.* **C51**, 38 (1995).
[7] S.C. Pieper, V.R. Pandharipande, R.B. Wiringa, J. Carlson, *Phys. Rev.* **C64**, 014001 (2001).
[8] J. Carlson *et al.*, `arXiv:1412.3081`.
[9] S.C. Pieper, *AIP Conf. Proc.* **1011**, 143 (2008).
[10] S.C. Pieper, R.B. Wiringa, *Annu. Rev. Nucl. Part. Sci.* **51**, 53 (2001).
[11] K.M. Nollett *et al.*, *Phys. Rev. Lett.* **99**, 022502 (2007).
[12] R. Schiavilla, R.B. Wiringa, S.C. Pieper, J. Carlson, *Phys. Rev. Lett.* **98**, 132501 (2007).
[13] B.S. Pudliner *et al.*, *Phys. Rev.* **C56**, 1720 (1997).
[14] R.B. Wiringa, S.C. Pieper, *Phys. Rev. Lett.* **89**, 182501 (2002).
[15] B.S. Pudliner, V.R. Pandharipande, J. Carlson, R.B. Wiringa, *Phys. Rev. Lett.* **74**, 4396 (1995).
[16] A. Akmal, V.R. Pandharipande, D.G. Ravenhall, *Phys. Rev.* **C58**, 1804 (1998).
[17] S. Gandolfi *et al.*, *Phys. Rev.* **C79**, 054005 (2009).
[18] S. Gandolfi, J. Carlson, S. Reddy, *Phys. Rev.* **C85**, 032801 (2012).
[19] A. Lovato *et al.*, *Phys. Rev. Lett.* **111**, 092501 (2013).
[20] A. Sarsa, S. Fantoni, K.E. Schmidt, F. Pederiva, *Phys. Rev.* **C68**, 024308 (2003).
[21] P. Maris *et al.*, *Phys. Rev.* **C87**, 054318 (2013).
[22] E. Epelbaum, H.W. Hammer, U.-G. Meißner, *Rev. Mod. Phys.* **81**, 1773 (2009).
[23] A. Gezerlis *et al.*, *Phys. Rev.* **C90**, 054323 (2014).
[24] A. Gezerlis *et al.*, *Phys. Rev. Lett.* **111**, 032501 (2013).
[25] J.E. Lynn *et al.*, *Phys. Rev. Lett.* **113**, 192501 (2014).
[26] A. Lovato *et al.*, *Phys. Rev. Lett.* **112**, 182502 (2014).
[27] S. Gandolfi, J. Carlson, S.C. Pieper, *Phys. Rev. Lett.* **106**, 012501 (2011).
[28] K.E. Schmidt, S. Fantoni, *Phys. Lett.* **B446**, 99 (1999).
[29] S. Gandolfi, A. Lovato, J. Carlson, K.E. Schmidt, *Phys. Rev.* **C90**, 061306(R) (2014).
[30] S. Gandolfi *et al.*, *Eur. Phys. J.* **A50**, 10 (2014).
[31] I. Tews, S. Gandolfi, A. Gezerlis, A. Schwenk, in preparation.
[32] D. Lonardoni, A. Lovato, S. Gandolfi, F. Pederiva, *Phys. Rev. Lett.* **114**, 092301 (2015).
[33] P.B. Demorest *et al.*, *Nature* **467**, 1081 (2010).
[34] J. Antoniadis *et al.*, *Science* **340**, 448 (2013).
[35] S. Gandolfi *et al.*, *Mon. Not. R. Astron. Soc.* **404**, L35 (2010).
[36] J.M. Lattimer M. Prakash, *Astrophys. J.* **550**, 426 (2001).
[37] A.W. Steiner, S. Gandolfi, *Phys. Rev. Lett.* **108**, 081102 (2012).
[38] A.W. Steiner, J.M. Lattimer, E.F. Brown, *Astrophys. J.* **722**, 33 (2010).